Finite temperature effects on anisotropic pressure and equation of state of dense neutron matter in an ultrastrong magnetic field

A. A. Isayev[1,2,*] and J. Yang[3,†]

[1]*Kharkov Institute of Physics and Technology, Academicheskaya Street 1, Kharkov, 61108, Ukraine*

[2]*Kharkov National University, Svobody Sq., 4, Kharkov, 61077, Ukraine*

[3]*Department of Physics and the Institute for the Early Universe, Ewha Womans University, Seoul 120-750, Korea*

(Received 30 September 2011; revised manuscript received 3 November 2011; published 12 December 2011)

Spin-polarized states in dense neutron matter with the recently developed Skyrme effective interaction (BSk20 parametrization) are considered in the magnetic fields H up to 10^{20} G at finite temperature. In a strong magnetic field, the total pressure in neutron matter is anisotropic, and the difference between the pressures parallel and perpendicular to the field direction becomes significant at $H > H_{\rm th} \sim 10^{18}$ G. The longitudinal pressure decreases with the magnetic field and vanishes in the critical field $10^{18} < H_c \lesssim 10^{19}$ G, resulting in the longitudinal instability of neutron matter. With increasing temperature, the threshold $H_{\rm th}$ and critical H_c magnetic fields also increase. The appearance of the longitudinal instability prevents the formation of a fully spin-polarized state in neutron matter and only the states with moderate spin polarization are accessible. The anisotropic equation of state is determined at densities and temperatures relevant to the interiors of magnetars. The entropy of strongly magnetized neutron matter turns out to be larger than the entropy of nonpolarized matter. This is caused by some specific details in the dependence of the entropy on the effective masses of neutrons with spin up and spin down in a polarized state.

DOI: 10.1103/PhysRevC.84.065802 PACS number(s): 21.65.Cd, 26.60.−c, 97.60.Jd, 21.30.Fe

I. INTRODUCTION

Magnetars are strongly magnetized neutron stars [1] with emissions powered by the dissipation of magnetic energy. According to one of the conjectures, magnetars can be the source of the extremely powerful short-duration γ-ray bursts [2–5]. The magnetic field strength at the surface of a magnetar is about 10^{14}–10^{15} G [6,7]. Such huge magnetic fields can be inferred from observations of magnetar periods and spin-down rates or from hydrogen spectral lines. In the interior of a magnetar the magnetic field strength may be even larger, reaching values of about 10^{18} G [8,9]. Under such circumstances, the issue of interest is the behavior of neutron star matter in a strong magnetic field [8–12].

A realistic description of neutron star matter should contain, at least, neutrons, protons, electrons, and muons subject to the charge neutrality and beta-equilibrium conditions. The magnetic field then influences the system properties through Pauli paramagnetism as well as via Landau quantization of the energy levels of charged particles. Nevertheless, because the neutron fraction is usually considered to be dominant, neutron star matter can be approximated by pure neutron matter as a first step toward a more realistic description of neutron stars. Such an approximation was used in the recent study [11] in the model consideration with the effective nuclear forces. It was shown that the behavior of spin polarization of neutron matter in the high-density region in a strong magnetic field crucially depends on whether neutron matter develops a spontaneous spin polarization (in the absence of a magnetic field) at several times the nuclear-matter saturation density, or the appearance of a spontaneous polarization is not allowed at the relevant densities (or delayed to much higher densities). The first case is usual for the Skyrme forces [13–23], while the second case is characteristic for the realistic nucleon-nucleon (NN) interaction [24–32]. In the former case, a ferromagnetic transition to a totally spin-polarized state occurs while, in the latter case, a ferromagnetic transition is excluded at all relevant densities and the spin polarization remains quite low even in the high-density region. If a spontaneous ferromagnetic transition is allowed, it was shown in the subsequent model consideration with the Skyrme effective forces [12] that the self-consistent equations for the spin polarization parameter at nonzero magnetic field have not only solutions corresponding to negative spin polarization (with the majority of neutron spins oriented opposite to the direction of the magnetic field) but, thanks to the strong spin-dependent medium correlations in the high-density region, also the solutions with positive spin polarization. In the last case, the formation of a metastable state with the majority of neutron spins oriented along the magnetic field is possible in the high-density interior of a neutron star.

The scenario for the evolution of spin polarization at high densities in which the spontaneous ferromagnetic transition in neutron matter is absent was considered for magnetic fields up to 10^{18} G [11]. Such an estimate for the limiting value of magnetic field strength in the core of a magnetar is usually obtained from the scalar virial theorem [33] based on Newtonian gravity. However, the density in the core of a magnetar is so large that the effects of general relativity might become important. Then, a further increase of the core magnetic field is expected above 10^{18} G [34]. By comparing with the observational x-ray data, it was argued that the interior magnetic field strength can be as large as 10^{19} G [35]. Also, it was shown in the recent study [36] that, in the core of

*isayev@kipt.kharkov.ua

†jyang@ewha.ac.kr

a magnetar, the magnetic field strength could reach values up to 10^{20} G, if to assume an inhomogeneous distribution of matter density and magnetic field inside the neutron star, or to allow the formation of a quark core in the high-density interior of a neutron star (concerning the last point, see also Ref. [37]). Under such circumstances, if to admit the interior magnetic fields with the strength $H > 10^{18}$ G, a different scenario is possible in which a field-induced ferromagnetic phase transition of neutron spins occurs in the magnetar core. This idea was investigated in the recent article [38], where it was shown within the framework of a lowest-constrained variational approach with the Argonne V_{18} NN potential that a fully spin-polarized state in neutron matter could be formed in a magnetic field $H \gtrsim 10^{19}$ G. Note, however, that, as was pointed out in Refs. [36,39], in such ultrastrong magnetic fields the breaking of the $\mathcal{O}(3)$ rotational symmetry by the magnetic field results in the anisotropy of the total pressure, having a smaller value parallel than perpendicular to the field direction. The possible outcome could be the gravitational collapse of a magnetar along the magnetic field, if the magnetic field strength is large enough. Thus, exploring the possibility of a field-induced ferromagnetic phase transition in neutron matter in a strong magnetic field, the effect of the pressure anisotropy has to be taken into account because this kind of instability could prevent the formation of a fully polarized state in neutron matter. This effect was not considered in Ref. [38], thus leaving open the possibility of the formation of a fully polarized state of neutron spins in a strong magnetic field. The degree of spin polarization is an important issue for determining the neutrino cross sections in the matter, and, hence, it is relevant for the adequate description of the neutrino transport and thermal evolution of a neutron star [17]. In the given study, we provide a fully self-consistent calculation of the thermodynamic quantities of spin-polarized neutron matter at finite temperature, taking into account the appearance of the pressure anisotropy in a strong magnetic field. We consider spin-polarization phenomena in a degenerate magnetized system of strongly interacting neutrons within the framework of a Fermi-liquid formalism [40–43], unlike to the previous works [36,39], where interparticle interactions were disregarded.

Note that, recently, new parametrizations of Skyrme forces were suggested, BSk19–BSk21 [44], which aimed to avoid the spontaneous spin instability of nuclear matter at densities beyond the nuclear saturation density for the case of zero temperature. This is achieved by adding different density-dependent terms to the standard Skyrme interaction. The BSk19 parametrization was constrained to reproduce the equation of state (EoS) of nonpolarized neutron matter [45] obtained in the variational calculation with the use of the realistic Urbana v_{14} NN potential and the three-body force called TNI. The BSk20 force corresponds to the stiffer EoS [46], obtained in the variational calculation with the use of the realistic Argonne V_{18} two-body potential and the semiphenomenological UIX* three-body force which includes also a relativistic-boost correction. Even a stiffer neutron matter EoS was suggested in the Brueckner-Hartree-Fock calculation of Ref. [47] based on the same V_{18} two-body potential and a more realistic three-body force containing different meson-exchange contributions. This EoS is the underlying one for the BSk21 Skyrme interaction. The advantage of all of these newly developed Skyrme forces is that they preserve the high-quality fits to the mass data obtained with the conventional Skyrme forces. An important quantity allowing one to distinguish between the different representatives of a generalized Skyrme interaction is the symmetry energy, which is defined as the difference between the energies per nucleon in neutron matter and symmetric nuclear matter (an alternative definition of the symmetry energy is also discussed in Ref. [44]). In the high-density region, the symmetry energy decreases with density for the BSk19 force, while it increases with density for BSk20 (moderately) and BSk21 (steeply) forces. As was clarified in Ref. [48] by testing almost 90 parametrizations of the conventional Skyrme forces, the Skyrme interactions, predicting the increasing behavior of the symmetry energy with density, put neutron star models in broad agreement with observations (e.g., providing a satisfactory description of the minimum rotation period, gravitational mass-radius relation, and the binding energy released in supernova collapse). Based on these arguments, one could consider a scenario, in which the symmetry energy increases with density in the high density region, to be more realistic. By this reason, in this study we will choose the BSk20 Skyrme parametrization for carrying out numerical calculations. Nevertheless, as emphasized in Ref. [44], only direct experimental evidence related to the high densities will allow one to ultimately decide which of the BSk19–BSk21 parametrizations of a generalized Skyrme interaction is more appropriate for the description of neutron-rich nuclear systems of astrophysical interest.

At this point, it is worth noting that we consider the thermodynamic properties of spin-polarized states in neutron matter in a strong magnetic field up to the high-density region relevant for astrophysics. Nevertheless, we take into account the nucleon degrees of freedom only, although other degrees of freedom such as pions, hyperons, kaons, or even quarks could be important at such high densities.

II. BASIC EQUATIONS

The normal (nonsuperfluid) states of neutron matter are described by the normal distribution function of neutrons $f_{\kappa_1\kappa_2} = \mathrm{Tr}\varrho a^+_{\kappa_2} a_{\kappa_1}$, where $\kappa \equiv (\mathbf{p}, \sigma)$, $\mathbf{p}$ is momentum, σ is the projection of spin on the third axis, and ϱ is the the density matrix of the system [21–23]. The energy of the system is specified as a functional of the distribution function f, $E = E(f)$, and determines the single-particle energy:

$$\varepsilon_{\kappa_1\kappa_2}(f) = \frac{\partial E(f)}{\partial f_{\kappa_2\kappa_1}}. \tag{1}$$

The self-consistent matrix equation for determining the distribution function f follows from the minimum condition of the thermodynamic potential [40,41] and is

$$\begin{aligned} f &= \{\exp(Y_0\varepsilon + Y_i\mu_n\sigma_i + Y_4) + 1\}^{-1} \\ &\equiv \{\exp(Y_0\xi) + 1\}^{-1}. \end{aligned} \tag{2}$$

Here the quantities ε, Y_i and Y_4 are matrices in the space of κ variables, with $(Y_{i,4})_{\kappa_1\kappa_2} = Y_{i,4}\delta_{\kappa_1\kappa_2}$, $Y_0 = 1/T$, $Y_i = -H_i/T$,

and $Y_4 = -\mu_0/T$ being the Lagrange multipliers, μ_0 being the chemical potential of neutrons, and T being the temperature. In Eq. (2), $\mu_n = -1.913\,042\,7\,(5)\mu_N$ is the neutron magnetic moment [49] (μ_N being the nuclear magneton) and σ_i are the Pauli matrices. Note that, unlike Refs. [12,50], the term with the external magnetic field $\mathbf{H}$ is not included in the single particle energy ε but is separately introduced in the exponent of the Fermi distribution (2).

Furthermore, it will be assumed that the third axis is directed along the external magnetic field $\mathbf{H}$. Given the possibility for alignment of neutron spins along or opposite to the magnetic field $\mathbf{H}$, the normal distribution function of neutrons and single-particle energy ε can be expanded in the Pauli matrices σ_i in spin space:

$$\begin{aligned} f(\mathbf{p}) &= f_0(\mathbf{p})\sigma_0 + f_3(\mathbf{p})\sigma_3, \\ \varepsilon(\mathbf{p}) &= \varepsilon_0(\mathbf{p})\sigma_0 + \varepsilon_3(\mathbf{p})\sigma_3. \end{aligned} \tag{3}$$

Using Eqs. (2) and (3), one can evidently express the distribution functions f_0 and f_3 in terms of the quantities ε:

$$f_0 = \tfrac{1}{2}\{n(\omega_+) + n(\omega_-)\}, \tag{4}$$

$$f_3 = \tfrac{1}{2}\{n(\omega_+) - n(\omega_-)\}. \tag{5}$$

Here $n(\omega) = \{\exp(Y_0\omega) + 1\}^{-1}$ and

$$\begin{aligned} \omega_\pm &= \xi_0 \pm \xi_3, \\ \xi_0 &= \varepsilon_0 - \mu_0, \xi_3 = -\mu_n H + \varepsilon_3. \end{aligned} \tag{6}$$

The quantity $\omega_\pm$, being the exponent in the Fermi distribution function n, plays the role of the quasiparticle spectrum. The branches $\omega_\pm$ correspond to neutrons with spin up and spin down, respectively.

The distribution functions f satisfy the normalization conditions

$$\frac{2}{\mathcal{V}}\sum_{\mathbf{p}} f_0(\mathbf{p}) = \varrho, \tag{7}$$

$$\frac{2}{\mathcal{V}}\sum_{\mathbf{p}} f_3(\mathbf{p}) = \varrho_\uparrow - \varrho_\downarrow \equiv \Delta\varrho. \tag{8}$$

Here $\varrho = \varrho_\uparrow + \varrho_\downarrow$ is the total density of neutron matter, $\varrho_\uparrow$ and $\varrho_\downarrow$ are the neutron number densities with spin up and spin down, respectively. The quantity $\Delta\varrho$ may be regarded as the neutron-spin order parameter which determines the magnetization of the system $M = \mu_n\Delta\varrho$. The spin ordering of neutrons can also be characterized by the spin-polarization parameter

$$\Pi = \frac{\Delta\varrho}{\varrho}.$$

The magnetization may contribute to the internal magnetic field $\mathbf{B} = \mathbf{H} + 4\pi\mathbf{M}$. However, we will assume, analogously to the previous studies [9,11,12], that, because of the tiny value of the neutron magnetic moment, the contribution of the magnetization to the inner magnetic field $\mathbf{B}$ remains small for all relevant densities and magnetic field strengths, and, hence,

$$\mathbf{B} \approx \mathbf{H}. \tag{9}$$

In order to get the self-consistent equations for the components of the single-particle energy, one has to set the energy functional of the system. It represents the sum of the matter and field energy contributions

$$E(f, H) = E_m(f) + E_f(H), \quad E_f(H) = \frac{H^2}{8\pi}\mathcal{V}. \tag{10}$$

The matter energy is the sum of the kinetic and Fermi-liquid interaction-energy terms [22,23]:

$$\begin{aligned} E_m(f) &= E_0(f) + E_{\rm int}(f), \\ E_0(f) &= 2\sum_{\mathbf{p}} \underline{\varepsilon}_0(\mathbf{p}) f_0(\mathbf{p}), \\ E_{\rm int}(f) &= \sum_{\mathbf{p}} \{\tilde{\varepsilon}_0(\mathbf{p}) f_0(\mathbf{p}) + \tilde{\varepsilon}_3(\mathbf{p}) f_3(\mathbf{p})\}, \end{aligned} \tag{11}$$

where

$$\tilde{\varepsilon}_0(\mathbf{p}) = \frac{1}{2\mathcal{V}}\sum_{\mathbf{q}} U_0^n(\mathbf{k}) f_0(\mathbf{q}), \quad \mathbf{k} = \frac{\mathbf{p}-\mathbf{q}}{2}, \tag{12}$$

$$\tilde{\varepsilon}_3(\mathbf{p}) = \frac{1}{2\mathcal{V}}\sum_{\mathbf{q}} U_1^n(\mathbf{k}) f_3(\mathbf{q}). \tag{13}$$

Here, $\underline{\varepsilon}_0(\mathbf{p}) = \frac{\mathbf{p}^2}{2m_0}$ is the free single-particle spectrum, m_0 is the bare mass of a neutron, $U_0^n(\mathbf{k})$ and $U_1^n(\mathbf{k})$ are the normal Fermi-liquid (FL) amplitudes, and $\tilde{\varepsilon}_0$, $\tilde{\varepsilon}_3$ are the FL corrections to the free single-particle spectrum. Using Eqs. (1) and (11), we get the self-consistent equations for the components of the single-particle energy in the form

$$\xi_0(\mathbf{p}) = \underline{\varepsilon}_0(\mathbf{p}) + \tilde{\varepsilon}_0(\mathbf{p}) - \mu_0, \quad \xi_3(\mathbf{p}) = -\mu_n H + \tilde{\varepsilon}_3(\mathbf{p}). \tag{14}$$

Taking into account expressions (4) and (5) for the distribution functions f_0 and f_3, solutions of the self-consistent Eqs. (14) should be found jointly with the normalization conditions (7) and (8).

The pressures (longitudinal and transverse with respect to the direction of the magnetic field) in the system are related to the diagonal elements of the stress tensor whose explicit expression reads [51]

$$\sigma_{ik} = \left[\tilde{\mathfrak{f}} - \varrho\left(\frac{\partial\tilde{\mathfrak{f}}}{\partial\varrho}\right)_{\mathbf{H},T}\right]\delta_{ik} + \frac{H_i B_k}{4\pi}. \tag{15}$$

Here,

$$\tilde{\mathfrak{f}} = \mathfrak{f}_H - \frac{H^2}{4\pi}, \tag{16}$$

$\mathfrak{f}_H = \frac{1}{\mathcal{V}}(E - TS) - \mathbf{HM}$ is the Helmholtz free energy density, and the entropy S is given by the formula

$$\begin{aligned} S &= -\sum_{\mathbf{p}}\sum_{\sigma=+,-} \{n(\omega_\sigma)\ln n(\omega_\sigma) + \bar{n}(\omega_\sigma)\ln\bar{n}(\omega_\sigma)\}, \\ \bar{n}(\omega) &= 1 - n(\omega). \end{aligned} \tag{17}$$

For the isotropic medium, the stress tensor (15) is symmetric. The transverse p_t and longitudinal p_l pressures are determined from the formulas

$$p_t = -\sigma_{11} = -\sigma_{22}, \quad p_l = -\sigma_{33}.$$

Hence, using Eqs. (10) and (15), one can get

$$p_t = \varrho\left(\frac{\partial f_m}{\partial \varrho}\right)_{H,T} - f_m + \frac{H^2}{8\pi}, \tag{18}$$

$$p_l = \varrho\left(\frac{\partial f_m}{\partial \varrho}\right)_{H,T} - f_m - \frac{H^2}{8\pi}, \tag{19}$$

where $f_m = \frac{1}{V}(E_m - TS)$ is the matter free energy density, and we disregarded in Eqs. (18) and (19) the terms proportional to M. The structure of the pressures p_t and p_l is different, which reflects the breaking of the rotational symmetry in the magnetic field. In ultrastrong magnetic fields, the term quadratic in the magnetic field (the Maxwell term) will dominate, leading to an increase in the transverse pressure and to a decrease in the longitudinal pressure. Hence, at some critical magnetic field, the longitudinal pressure will vanish, resulting in the longitudinal instability of neutron matter. Obviously, at finite temperature the pressures p_t and p_l will be larger compared to the zero-temperature case, and, hence, an increase in the temperature will lead to an increase in the critical magnetic field. Here we would like to find the magnitude of the critical field at temperatures of a few tens of MeV, which can be relevant for protoneutron stars, and also to determine the corresponding maximum degree of spin polarization in neutron matter.

III. SPIN POLARIZATION AT $H = 0$, $T \neq 0$

To provide numerical calculations, we use the BSk20 Skyrme interaction [44] developed to reproduce the zero-temperature microscopic EoS of nonpolarized neutron matter [46]. Although spontaneous spin polarization at zero temperature is missing for this parametrization for all relevant densities, it is not excluded that, at finite temperature, a spontaneous ferromagnetic phase transition could occur. Actually, this is the case as will be shown later. In the model calculations of this section we consider temperatures somewhat larger than the temperatures which could be reachable in the interior of protoneutron stars [52]. This will help us to find the critical temperature above which a spontaneous polarization appears, and will also allow us to determine the relevant temperature range for studying spin polarization at $H \neq 0$.

The recently developed parametrizations BSk19–BSk21 of the Skyrme effective forces appear as a generalization of Skyrme effective NN interaction of the conventional form. In the conventional case, the amplitude of Skyrme NN interaction reads [53]

$$\hat{v}(\mathbf{p},\mathbf{q}) = t_0(1 + x_0P_\sigma) + \frac{1}{6}t_3(1 + x_3P_\sigma)\varrho^\alpha + \frac{1}{2\hbar^2}t_1(1 + x_1P_\sigma)(\mathbf{p}^2 + \mathbf{q}^2) + \frac{t_2}{\hbar^2}(1 + x_2P_\sigma)\mathbf{pq}, \tag{20}$$

where $P_\sigma = (1 + \boldsymbol{\sigma}_1\boldsymbol{\sigma}_2)/2$ is the spin exchange operator, t_i, x_i and α are some phenomenological parameters specifying a given parametrization of the Skyrme interaction. The Skyrme interaction used in Ref. [44] has the form

$$\hat{v}'(\mathbf{p},\mathbf{q}) = \hat{v}(\mathbf{p},\mathbf{q}) + \frac{\varrho^\beta}{2\hbar^2}t_4(1 + x_4P_\sigma)(\mathbf{p}^2 + \mathbf{q}^2) + \frac{\varrho^\gamma}{\hbar^2}t_5(1 + x_5P_\sigma)\mathbf{pq}. \tag{21}$$

In Eq. (21), two additional terms are the density-dependent generalizations of the t_1 and t_2 terms of the usual form. Specific values of the parameters t_i, x_i, α, β, and γ for Skyrme forces BSk19–BSk21 are given in Table I [44].

TABLE I. Parameters of BSk19–BSk21 Skyrme forces, according to Ref. [44]. The value of the nuclear saturation density ϱ_0 is shown in the bottom line.

	BSk19	BSk20	BSk21
t_0 [MeV fm^3]	−4115.21	−4056.04	−3961.39
t_1 [MeV fm^5]	403.072	438.219	396.131
t_2 [MeV fm^5]	0	0	0
t_3 [MeV fm$^{3+3\alpha}$]	23670.4	23256.6	22588.2
t_4 [MeV fm$^{5+3\beta}$]	−60.0	−100.000	−100.000
t_5 [MeV fm$^{5+3\gamma}$]	−90.0	−120.000	−150.000
x_0	0.398848	0.569613	0.885231
x_1	−0.137960	−0.392047	0.0648452
t_2x_2 [MeV fm^5]	−1055.55	−1147.64	−1390.38
x_3	0.375201	0.614276	1.03928
x_4	−6.0	−3.00000	2.00000
x_5	−13.0	−11.0000	−11.0000
α	1/12	1/12	1/12
β	1/3	1/6	1/2
γ	1/12	1/12	1/12
ϱ_0 [fm^{-3}]	0.1596	0.1596	0.1582

In Ref. [41,43]. As follows from Eqs. (20) and (21), in order to obtain the corresponding expressions for the generalized Skyrme interaction (21), one should use the substitutions

$$t_1 \to t_1 + t_4\varrho^\beta, \quad t_1x_1 \to t_1x_1 + t_4x_4\varrho^\beta, \tag{22}$$

$$t_2 \to t_2 + t_5\varrho^\gamma, \quad t_2x_2 \to t_2x_2 + t_5x_5\varrho^\gamma. \tag{23}$$

Therefore, the FL amplitudes are related to the parameters of the Skyrme interaction (21) by formulas [54]

$$U_0^n(\mathbf{k}) = 2t_0(1 - x_0) + \frac{t_3}{3}\varrho^\alpha(1 - x_3) + \frac{2}{\hbar^2}[t_1(1 - x_1) + t_4(1 - x_4)\varrho^\beta + 3t_2(1 + x_2) + 3t_5(1 + x_5)\varrho^\gamma]\mathbf{k}^2, \tag{24}$$

$$U_1^n(\mathbf{k}) = -2t_0(1 - x_0) - \frac{t_3}{3}\varrho^\alpha(1 - x_3) + \frac{2}{\hbar^2}[t_2(1 + x_2) + t_5(1 + x_5)\varrho^\gamma - t_1(1 - x_1) - t_4(1 - x_4)\varrho^\beta]\mathbf{k}^2. \tag{25}$$

Now we present the results of the numerical solution of the self-consistent equations at $H = 0$ with the BSk20 Skyrme force. Figure 1 shows the spin-polarization parameter

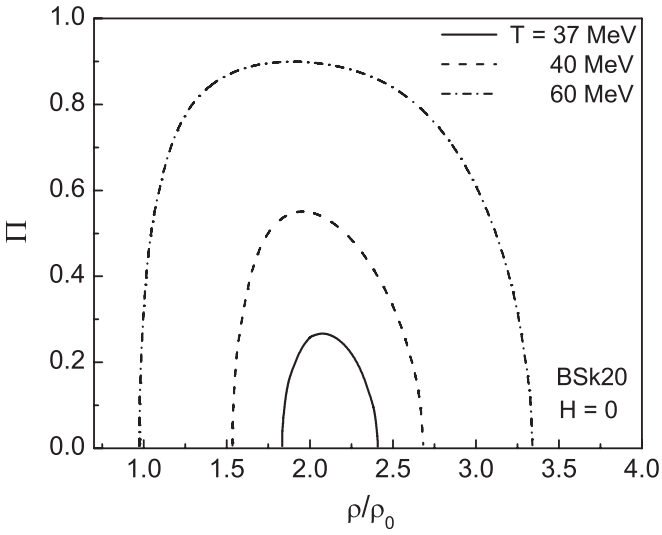

FIG. 1. Neutron spin-polarization parameter as a function of the density for BSk20 Skyrme force at $H = 0$ and several fixed values of temperature.

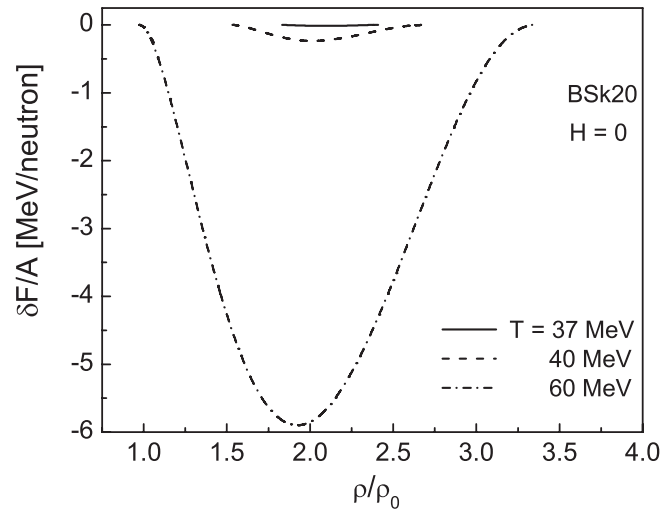

FIG. 2. Difference between the free energies per neutron of spin-polarized and nonpolarized states as a function of the density at $H = 0$ and several fixed values of the temperature for the BSk20 Skyrme force. The difference is shown only for the density domains where spontaneous polarization exists.

of neutron matter as a function of the density for a few fixed values of the temperature of several tens of MeV. At zero temperature, there is no spontaneous polarization at all relevant densities because two additional terms in a generalized form (21) of the Skyrme interaction were constrained just with the aim to exclude a nonzero polarization at vanishing temperature. Spontaneous polarization does not appear up to some critical temperature T_c which is, at least, larger than 35 MeV. Beyond T_c, spontaneous spin polarization exists in a finite-density interval $(\varrho_{c_1}, \varrho_{c_2})$. The unexpected moment is that the temperature promotes spontaneous spin polarization, increasing both the width of the density domain where a nonzero polarization exists and the magnitude of the spin-polarization parameter. In particular, if to approach the density interval $(\varrho_{c_1}, \varrho_{c_2})$ from the lower densities, then the left critical point ϱ_{c_1}, at which spontaneous polarization appears, decreases with temperature, contrary to intuition which suggests that the temperature should act as a preventing factor to spin polarization and, hence, should delay its appearance. Analogously, with increasing temperature the right critical point ϱ_{c_2} for the disappearance of spontaneous polarization should, according to intuition, decrease, contrary to what really occurs (i.e., the critical density ϱ_{c_2} increases with temperature).

In order to clarify whether a spontaneously spin-polarized state is thermodynamically preferable over the nonpolarized state, one should compare the corresponding free energies. Figure 2 shows the difference between the free energies per neutron of spin-polarized and nonpolarized states, $\delta F/A = [F(\varrho, T, \Pi(\varrho, T)) - F(\varrho, T, \Pi = 0)]/A$, as a function of the density at the same fixed temperatures considered above. It is seen that a spontaneously polarized state is preferable over the nonpolarized state for all relevant densities and temperatures where spontaneous polarization exists. With increasing temperature, the minimum of the difference $\delta F/A$ becomes more pronounced and, hence, a spontaneously polarized state becomes more stable with respect to the nonpolarized one. Thus, the state with spontaneous polarization, described by the spin-polarization parameter with such unusual properties (cf. Fig. 1), is supported thermodynamically by the balance of the free energies.

In order to get a deeper insight into the problem, let us consider separate contributions to the difference between the free energies per neutron $\delta F/A = \delta E/A - T\delta S/A$. Figure 3 shows the difference between the energies per neutron of spin-polarized and nonpolarized states, $\delta E/A = [E(\varrho, T, \Pi(\varrho, T)) - E(\varrho, T, \Pi = 0)]/A$, as a function of the density at the same fixed temperatures considered above. It is seen that the energy per neutron of a spin-polarized state is always larger than that of the nonpolarized state for the density domain where spontaneous spin polarization exists. This is because increasing the temperature and spin polarization leads to increasing the kinetic energy term in the energy functional of

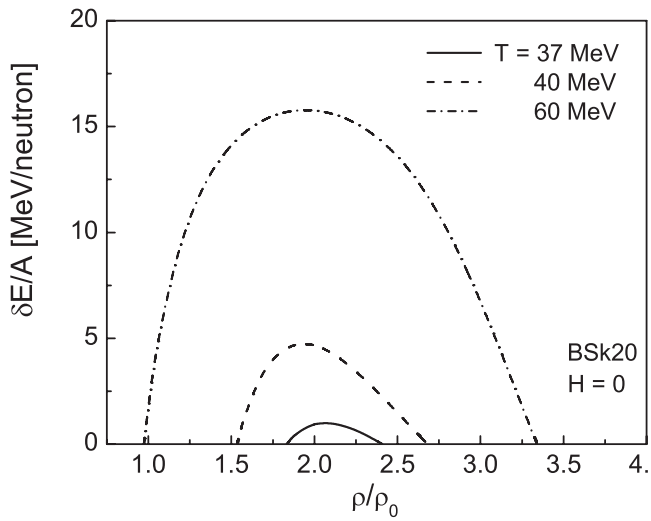

FIG. 3. Same as in Fig. 2 but for the difference between the energies per neutron of spin-polarized and nonpolarized states.

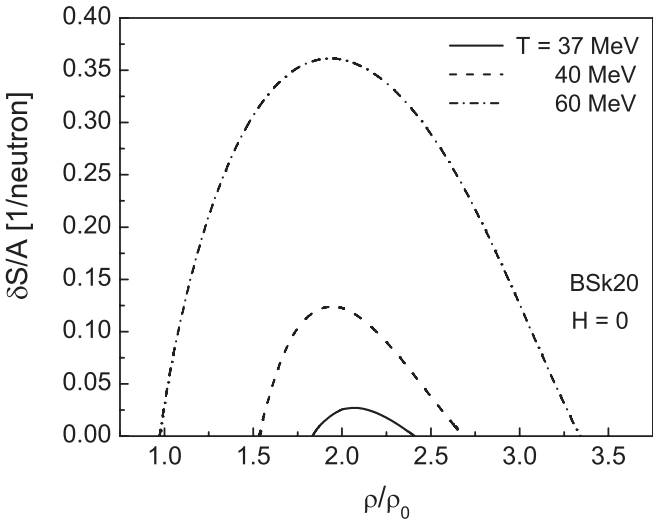

FIG. 4. Same as in Fig. 2 but for the difference between the entropies per neutron of spin-polarized and nonpolarized states.

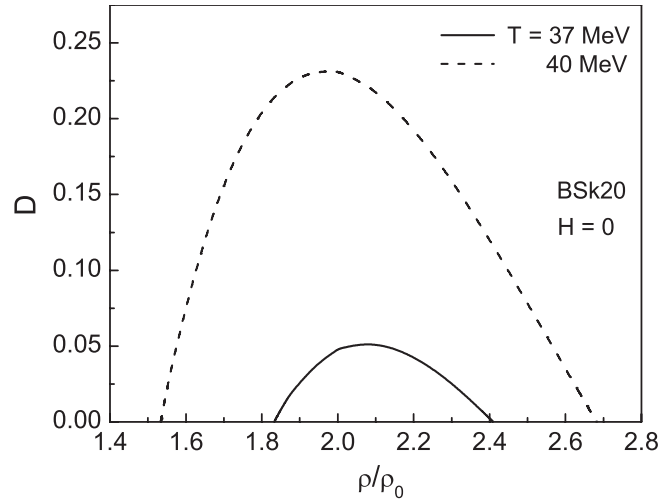

FIG. 5. Difference D in constraint (27) for the branch Π of spontaneous polarization as a function of density at $T = 37$ MeV and $T = 40$ MeV for the BSk20 Skyrme force.

the system. The sign of the difference $\delta E/A$ could, in principle, be inverted by the negative contribution of the term in the energy functional (11) describing spin correlations in neutron matter with nonzero polarization, but that is not, however, the case. Therefore, the inequality $\delta F/A < 0$ can hold only because of the inequality $\delta S/A > 0$ for the density range where spontaneous polarization exists. Figure 4 shows that this is actually true, and the entropy per neutron of a spin-polarized state is larger than that of the nonpolarized state for the corresponding temperatures and densities. This unexpected behavior contradicts intuition which suggests that the entropy of a more-ordered spin-polarized state should be less than that of the nonpolarized state. Note that such unusual behavior of the entropy of a spin-polarized state was found earlier for neutron matter with the Skyrme effective interaction [55] and for symmetric nuclear matter with the Gogny effective interaction [56,57] (in the latter case, for antiferromagnetically ordered nucleon spins). The difference, however, is that, in these earlier studies, instability with respect to spontaneous spin ordering occurred already at zero temperature whereas in the given case it appears only at temperatures larger than the critical temperature. Also, it was clarified earlier [55,57] that the unusual behavior of the entropy of a spin-polarized state should be traced back to its dependence on the effective masses of spin-up and spin-down nucleons and to a violation of a certain constraint on them at the corresponding temperatures and densities. In Ref. [55], this constraint was formulated for totally polarized neutron matter and in Ref. [57] for symmetric nuclear matter with arbitrary antiferromagnetic spin polarization.

Let us verify now whether this holds true in our case. In the low-temperature limit the entropy per neutron is given by

$$S/A = \sum_{\sigma=+,-} \frac{\pi^2}{2\varepsilon_{F\sigma}} T, \tag{26}$$

where $\varepsilon_\sigma = \frac{\hbar^2 k_{F\sigma}^2}{2m_\sigma}$ is the Fermi energy of neutrons with spin up and spin down, and $k_\sigma = (6\pi^2 \varrho_\sigma)^{1/3}$ is the respective Fermi momentum. The low-temperature expansion (26) is valid until $T/\varepsilon_{F\sigma} \ll 1$. By requiring the difference between the entropies of spin-polarized and nonpolarized states to be negative, one can derive the following constraint on the effective masses $m_{n\uparrow}$ and $m_{n\downarrow}$ of neutrons with spin up and spin down in a spin-polarized state [50]:

$$D \equiv \frac{m_{n\uparrow}}{m_n}(1+\Pi)^{\frac{1}{3}} + \frac{m_{n\downarrow}}{m_n}(1-\Pi)^{\frac{1}{3}} - 2 < 0, \tag{27}$$

where

$$\begin{aligned}\frac{\hbar^2}{2m_{\uparrow(\downarrow)}} = \frac{\hbar^2}{2m_0} &+ \frac{\varrho_{\uparrow(\downarrow)}}{2}[t_2(1+x_2) + t_5(1+x_5)\varrho^\gamma] \\ &+ \frac{\varrho_{\downarrow(\uparrow)}}{4}[t_1(1-x_1) + t_4(1-x_4)\varrho^\beta \\ &+ t_2(1+x_2) + t_5(1+x_5)\varrho^\gamma].\end{aligned} \tag{28}$$

In the constraint (27), the effective mass m_n of a neutron in nonpolarized neutron matter is given by [54]

$$\begin{aligned}\frac{\hbar^2}{2m_n} = \frac{\hbar^2}{2m_0} &+ \frac{\varrho}{8}[t_1(1-x_1) + t_4(1-x_4)\varrho^\beta \\ &+ 3t_2(1+x_2) + 3t_5(1+x_5)\varrho^\gamma].\end{aligned} \tag{29}$$

After the self-consistent determination of the spin-polarization parameter, one can check whether inequality (27) is satisfied at the corresponding densities and temperatures. Figure 5 shows the left-hand side D of the constraint (27) for the branch $\Pi(\varrho, T)$ of spontaneous polarization as a function of the density at the temperatures $T = 37$ MeV and $T = 40$ MeV, where the accuracy of the approximation $T/\varepsilon_{F\sigma} \ll 1$ is satisfactory. It is seen that inequality (27) is violated, implying that the entropy of a spontaneously polarized state is larger than the entropy of the nonpolarized state at the respective densities and temperatures. Hence, the unusual behavior of the entropy of a spontaneously polarized state mentioned above can be related to the peculiarities of its dependence on the effective masses of neutrons with spin up and spin down. A nontrivial character of the density dependence of the effective masses

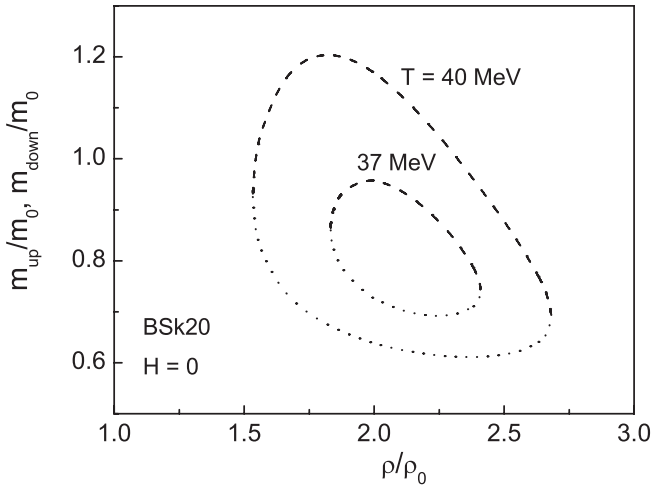

FIG. 6. Ratio of effective mass of a neutron with spin up (upper dashed curves) and spin down (lower dotted curves) in a spontaneously polarized state to bare neutron mass as a function of density at $T = 37$ MeV and $T = 40$ MeV for the BSk20 Skyrme force.

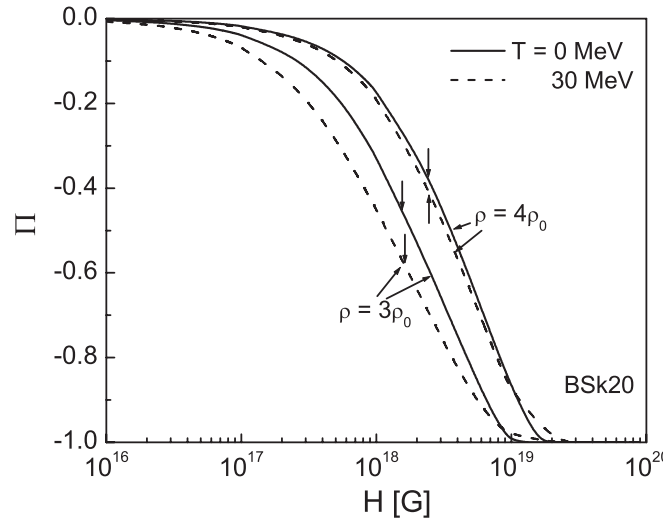

FIG. 7. Neutron spin-polarization parameter as a function of the magnetic field strength for the BSk20 Skyrme force at $T = 0$ and $T = 30$ MeV, and at two fixed densities, $\varrho = 3\varrho_0$ and $\varrho = 4\varrho_0$. The vertical arrows indicate the maximum magnitude of spin polarization attainable at the given temperature and density; see further details in the text.

$m_{n\uparrow}$ and $m_{n\downarrow}$ in neutron matter with spontaneous polarization at different temperatures is clearly seen from Fig. 6.

In the subsequent analysis, following the scenario according to which spontaneous polarization should be avoided at the relevant densities and temperatures, we will confine our analysis to temperatures up to 30 MeV which are definitely less than the critical temperature $T_c \gtrsim 35$ MeV. Such a choice of the relevant temperature interval is consistent with the results of completely independent research [52] of hybrid stars in the context of relativistic mean-field theory, according to which the maximum temperature attainable in their interior does not exceed 35 MeV.

IV. LONGITUDINAL AND TRANSVERSE PRESSURES AT FINITE TEMPERATURE. ANISOTROPIC EoS

In this section, we will study the influence of finite temperatures on thermodynamic quantities of spin-polarized neutron matter in an ultrastrong magnetic field. We will take into account the effects of the pressure anisotropy, and, in particular, will clarify to which extent the critical magnetic field, at which the longitudinal instability in magnetized neutron matter occurs, will increase due to the impact of finite temperatures.

First, we present the results of the numerical solution of the self-consistent equations. Figure 7 shows the spin-polarization parameter of neutron matter as a function of the magnetic field H at two different temperatures, $T = 0$ and $T = 30$ MeV, and at two different values of the neutron matter density, $\varrho = 3\varrho_0$ and $\varrho = 4\varrho_0$, which can be relevant for the central regions of a magnetar. Under increasing the density, the effect produced by the magnetic field on spin polarization of neutron matter becomes smaller. It is seen that the impact of the magnetic field remains insignificant up to the field strength $H \sim 10^{17}$ G. At the magnetic field $H = 10^{18}$ G, usually considered to be the maximum magnetic field strength in the core a magnetar (according to a scalar virial theorem [33]), the magnitude of the spin-polarization parameter does not exceed 45% at $\varrho = 3\varrho_0$ and 19% at $\varrho = 4\varrho_0$ (for the temperatures under consideration). However, the situation changes if larger magnetic fields are allowable: Upon further increasing the magnetic field strength, the magnitude of the spin-polarization parameter increases and spin polarization approaches its limiting value $\Pi = -1$, corresponding to a fully spin-polarized state. For example, a fully polarized state is formed at $H \approx 1.3 \times 10^{19}$ G for the temperature $T = 0$ MeV and at $H \approx 2.3 \times 10^{19}$ G for $T = 30$ MeV at $\varrho = 3\varrho_0$ (i.e., certainly for magnetic fields $H \gtrsim 10^{19}$ G). Note that we speak about a fully polarized state at finite temperature although some quantity of neutrons with spin up are always present at $T \neq 0$. Nevertheless, this quantity may be made arbitrarily small by further increasing the magnetic field, and we consider that a fully polarized state is formed if the deviation from the limiting value $\Pi = -1$ is less than 10^{-4}. Upon increasing the temperature, the value of the magnetic field, at which a fully polarized state occurs, increases, as one could expect. However, practically up to magnetic fields of about 10^{19} G, spin polarization demonstrates the unusual behavior and increases with temperature. Furthermore, it will be shown that this behavior is thermodynamically supported by the corresponding balance of the Helmholtz free energies. The meaning of the vertical arrows in Fig. 7 is explained later in the text.

Now, we should check whether a fully spin-polarized state of neutrons in a strong magnetic field can indeed be formed by calculating the anisotropic pressure in dense neutron matter. Figure 8(a) shows the pressures (longitudinal and transverse) in neutron matter as functions of the magnetic field H at the same fixed temperatures and densities as considered above. The upper branches in the branching curves correspond to the transverse pressure, the lower ones to the longitudinal pressure.

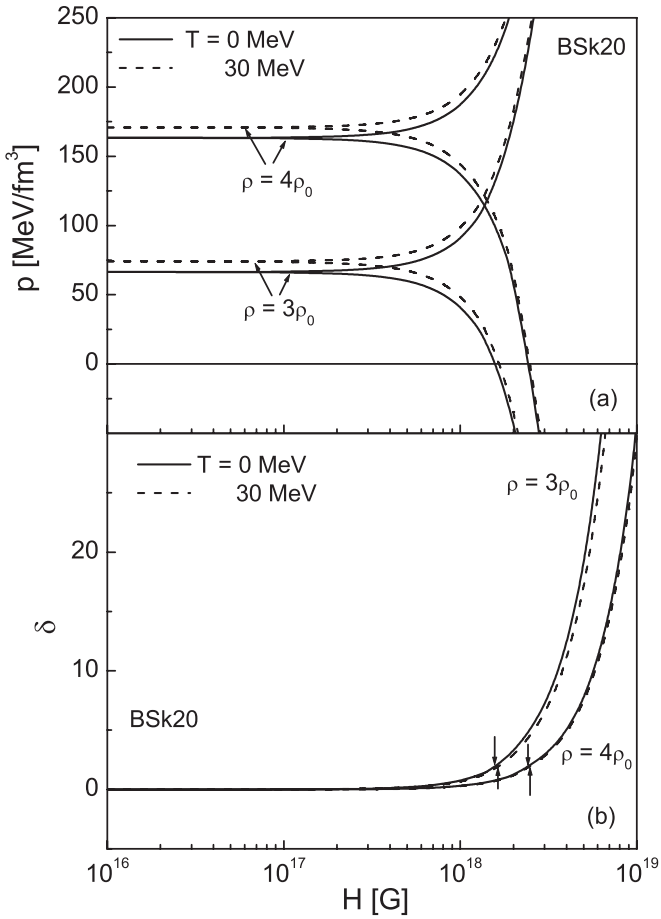

FIG. 8. Same as in Fig. 7 but for (a) the pressures, longitudinal (descending branches) and transverse (ascending branches). (b) Same as in the top panel but for the normalized difference between the transverse and longitudinal pressures. The vertical arrows in the lower panel indicate the points corresponding to the onset of the longitudinal instability in neutron matter.

First of all, it is clearly seen that, up to some threshold magnetic field, the difference between the transverse and longitudinal pressures is unessential that corresponds to the isotropic regime. Beyond this threshold magnetic field strength, the anisotropic regime holds for which the transverse pressure increases with H while the longitudinal pressure decreases. The increase in temperature leads to the increase in the pressures transverse p_t and longitudinal p_l. Also, the increase in density has the same effect on the pressures p_t and p_l as the increase in temperature. The most important feature is that the longitudinal pressure vanishes at some critical magnetic field H_c marking the onset of the longitudinal instability in neutron matter. For example, $H_c \approx 1.56 \times 10^{18}$ G for $T = 0$ MeV and $H_c \approx 1.64 \times 10^{18}$ G for $T = 30$ MeV at $\varrho = 3\varrho_0$, and $H_c \approx 2.42 \times 10^{18}$ G for $T = 0$ MeV and $H_c \approx 2.48 \times 10^{18}$ G for $T = 30$ MeV at $\varrho = 4\varrho_0$. Hence, at the finite temperatures relevant for protoneutron stars, the critical magnetic field is increased compared to the zero-temperature case but this increase is, in fact, insignificant. Even accounting for the finite-temperature effects, the critical field does not exceed 10^{19} G for the density range under consideration.

The magnitude of the spin-polarization parameter Π also cannot exceed some limiting value corresponding to the critical field H_c. These maximum values of the magnitude of Π are shown in Fig. 7 by the vertical arrows. In particular, $\Pi_c \approx -0.46$ for $T = 0$ MeV and $\Pi_c \approx -0.58$ for $T = 30$ MeV at $\varrho = 3\varrho_0$, and $\Pi_c \approx -0.38$ for $T = 0$ MeV and $\Pi_c \approx -0.41$ for $T = 30$ MeV at $\varrho = 4\varrho_0$. As can be inferred from these values, the appearance of negative longitudinal pressure in an ultrastrong magnetic field prevents the formation of a fully polarized spin state in the core of a magnetar. Therefore, only the onset of a field-induced ferromagnetic phase transition, or its near vicinity, can be caught under increasing magnetic field strength in dense neutron matter at finite temperature. A complete spin polarization in the magnetar core is not allowed by the appearance of negative pressure along the direction of the magnetic field, contrary to the conclusion of Ref. [38] where the pressure anisotropy in a strong magnetic field was disregarded.

Figure 8(b) shows the difference between the transverse and longitudinal pressures normalized to the value of the pressure p_0 in the isotropic regime (which corresponds to the weak field limit with $p_l = p_t = p_0$):

$$\delta = \frac{p_t - p_l}{p_0}.$$

Applying the criterion $\delta \simeq 1$ for the transition from the isotropic regime to the anisotropic regime, the transition occurs at the threshold field $H_{\rm th} \approx 1.15 \times 10^{18}$ G for $T = 0$ MeV and $H_{\rm th} \approx 1.22 \times 10^{18}$ G for $T = 30$ MeV at $\varrho = 3\varrho_0$, and at $H_{\rm th} \approx 1.83 \times 10^{18}$ G for $T = 0$ MeV and $H_{\rm th} \approx 1.86 \times 10^{18}$ G for $T = 30$ MeV at $\varrho = 4\varrho_0$. In all cases under consideration, the threshold field $H_{\rm th}$ is greater than 10^{18} G and, hence, the isotropic regime holds for the fields up to 10^{18} G. For comparison, the threshold field for a relativistic dense gas of free charged fermions at zero temperature was found to be about 10^{17} G [36] (without including the anomalous magnetic moments of fermions). For a degenerate gas of free neutrons at zero temperature the model-dependent estimate gives $H_{\rm th} \simeq 4.5 \times 10^{18}$ G [39] (including the neutron anomalous magnetic moment). The normalized splitting of the transverse and longitudinal pressures increases more rapidly with magnetic field at smaller density and/or at lower temperature. The vertical arrows in Fig. 8(b) indicate the points corresponding to the onset of the longitudinal instability in neutron matter. Since the threshold field $H_{\rm th}$ is less than the critical field H_c for the appearance of the longitudinal instability, the anisotropic regime can be relevant for the core of a magnetar. The maximum allowable normalized splitting of the pressures corresponding to the critical field H_c is $\delta \sim 2$. If the anisotropic regime sets in, a neutron star has the oblate form. Thus, as follows from the preceding discussions, in the anisotropic regime the pressure anisotropy plays an important role in determining the spin structure and configuration of a neutron star.

At the given thermodynamic variables ϱ, T, and H, the Helmholtz free energy is a relevant thermodynamic function whose minimum determines a state of thermodynamic equilibrium. Figure 9(a) shows the Helmholtz free energy density of the system as a function of the magnetic field

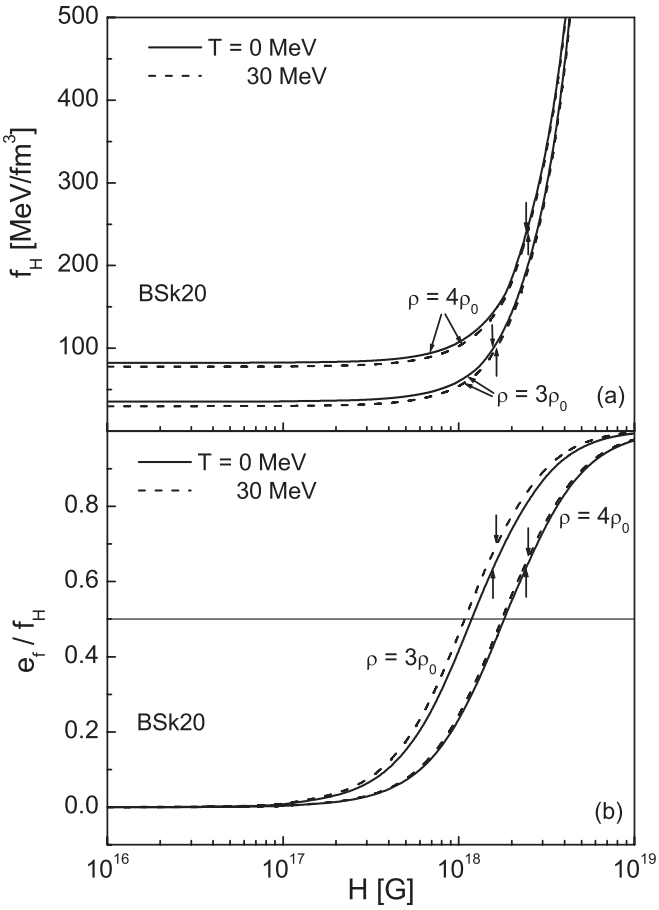

FIG. 9. (a) Same as in Fig. 7 but for the Helmholtz free energy density of the system. (b) Same as in Fig. 7 but for the ratio of the magnetic field energy density to the Helmholtz free energy density of the system. The meaning of the vertical arrows is the same as in Fig. 8(b).

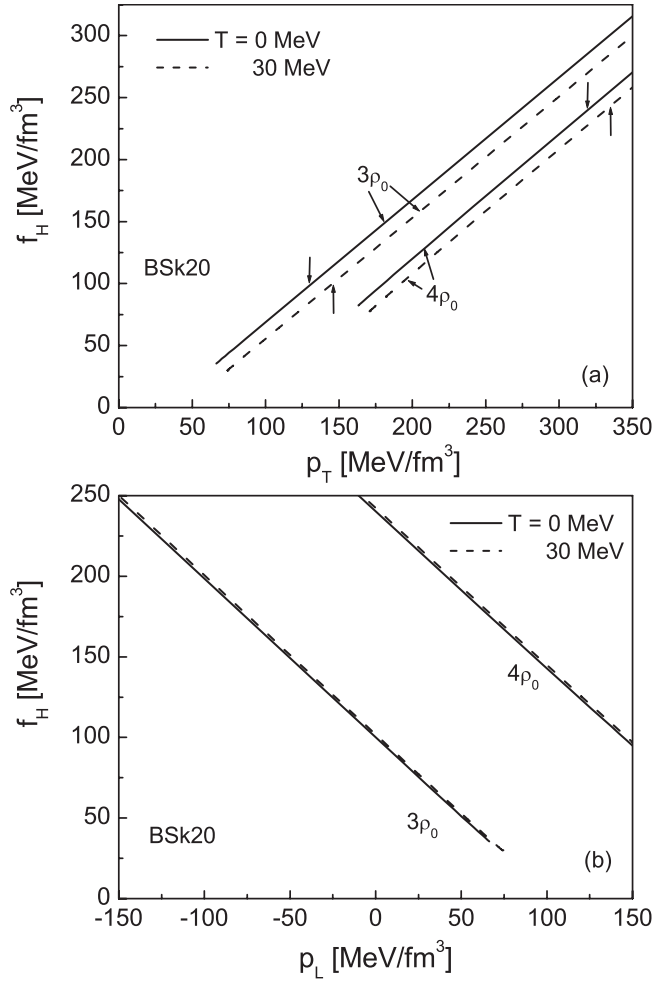

FIG. 10. Helmholtz free energy density of the system as a function of (a) the transverse pressure p_t, (b) the longitudinal pressure p_l at $T = 0$ (solid lines) and $T = 30$ MeV (dashed lines), and at two fixed densities, $\varrho = 3\varrho_0$ and $\varrho = 4\varrho_0$. The meaning of the vertical arrows in the top panel is the same as in Fig. 8(b). In the bottom panel, the physical region corresponds to $p_l > 0$.

H at two fixed temperatures, $T = 0$ and $T = 30$ MeV, and at two different densities, $\varrho = 3\varrho_0$ and $\varrho = 4\varrho_0$. It is seen that magnetic fields up to $H \sim 10^{18}$ G have practically small effects on the Helmholtz free energy density f_H, but beyond this field strength the contribution of the magnetic field energy to the free energy f_H rapidly increases with H. However, this increase is limited by the values of the critical magnetic field corresponding to the onset of the longitudinal instability in neutron matter. The respective points on the curves are indicated by the vertical arrows.

Figure 9(b) shows the ratio of magnetic field energy density $e_f = \frac{H^2}{8\pi}$ to Helmholtz free energy density under the same assumptions as for Fig. 9(a). The intersection points of the respective curves in this panel with the line $e_f/f_H = 0.5$ correspond to the magnetic fields at which the matter and field contributions to the Helmholtz free energy density are equal. This happens at $H \approx 1.18 \times 10^{18}$ G for $T = 0$ MeV and $H \approx 1.08 \times 10^{18}$ G for $T = 30$ MeV at $\varrho = 3\varrho_0$, and at $H \approx 1.81 \times 10^{18}$ G for $T = 0$ MeV and $H \approx 1.76 \times 10^{18}$ G for $T = 30$ MeV at $\varrho = 4\varrho_0$. These values are quite close to the respective values of the threshold field $H_{\rm th}$ and, hence, the transition to the anisotropic regime occurs at the magnetic field strength at which the field and matter contributions to the Helmholtz free energy density become equally important. It is also seen from Fig. 9(b) that, in all cases when the longitudinal instability occurs in the magnetic field H_c the contribution of the magnetic field energy density to the Helmholtz free energy density of the system dominates over the matter contribution.

Because of the pressure anisotropy, the EoS of neutron matter in a strong magnetic field is also anisotropic. Figure 10 shows the dependence of the Helmholtz free energy density f_H on the transverse pressure (top panel) and on the longitudinal pressure (bottom panel) after excluding the dependence on H in these quantities. Since the dominant Maxwell term enters the pressure p_t and free energy density f_H with a positive sign, and enters the pressure p_l with a negative sign, the free energy density f_H is the increasing function of p_t and decreasing function of p_l. In the case of $f_H(p_t)$ dependence, at the given density, the same p_t corresponds to the larger magnetic field H at the temperature $T = 0$ MeV compared to the $T = 30$ MeV case [see Fig. 8(a)]. The overall effect of the two factors

(temperature and magnetic field) will be the larger value of the free energy density f_H at the given p_t and density for the temperature $T = 0$ MeV compared with the $T = 30$ MeV case [see Fig. 10(a)]. The analogous arguments show that, at the given temperature and p_t, the Helmholtz free energy density is larger for the smaller density. In the case of $f_H(p_l)$ dependence, at the given density, the same p_l corresponds to the smaller magnetic field H for the temperature $T = 0$ MeV compared to the $T = 30$ MeV case [see Fig. 8(a)]. Hence, the free energy density f_H at the given p_l and density is larger for the temperature $T = 30$ MeV than that for the $T = 0$ MeV case [see Fig. 10(b)]. Analogously, at the given temperature and p_l, the free energy density f_H is larger for the larger density. In the bottom panel, the physical region corresponds to the positive values of the longitudinal pressure.

It is worth noting at this point that, since the EoS of neutron matter becomes highly anisotropic in an ultrastrong magnetic field, the usual scheme for finding the mass-radius relationship based on the Tolman-Oppenheimer-Volkoff (TOV) equations [58] for a spherically symmetric and static neutron star should be revised. Instead of this, the corresponding relationship should be found by the self-consistent treatment of the anisotropic EoS and axisymmetric TOV equations substituting the conventional TOV equations in the case of an axisymmetric neutron star.

V. UNUSUAL BEHAVIOR OF ENTROPY at $H \neq 0$

As was discussed in the previous section, the magnitude of the spin-polarization parameter increases with temperature in fields up to about 10^{19} G. The Helmholtz free energy density f_H, whose minimum at the given ϱ, T, H determines the state of a thermodynamic equilibrium, decreases with temperature [cf. Fig. 9(a)] and, hence, such an unusual behavior of spin polarization with temperature is supported thermodynamically. The Helmholtz free energy density f_H can be decomposed into the matter and field contributions,

$$f_H = f_{Hm} + e_f,$$

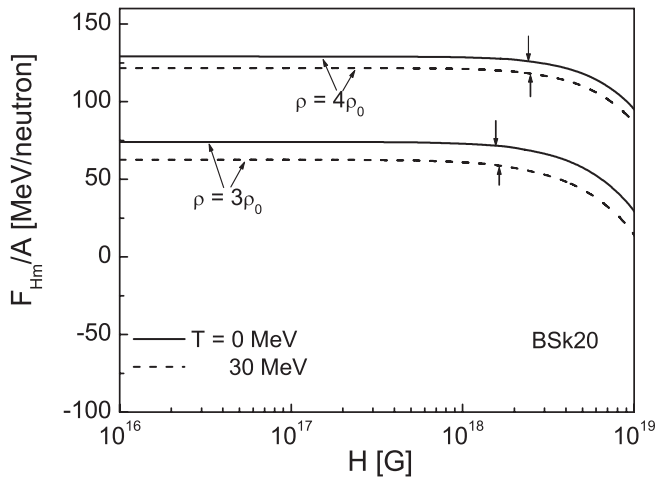

FIG. 11. Same as in Fig. 7 but for the matter part F_{Hm}/A of the Helmholtz free energy per neutron. The meaning of the vertical arrows is the same as in Fig. 8(b).

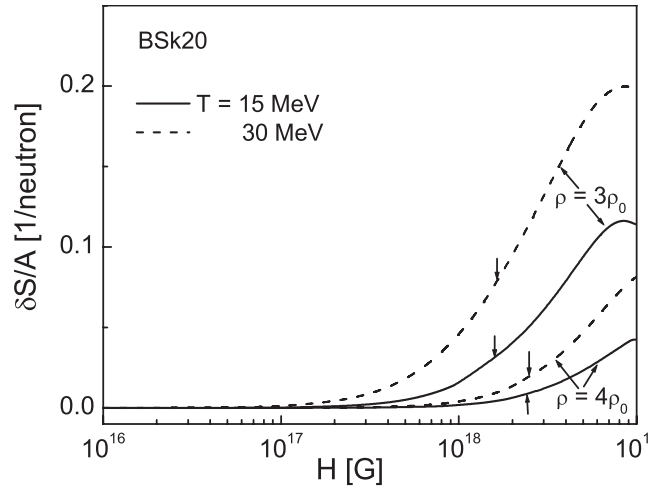

FIG. 12. Difference between entropies per neutron of magnetized neutron matter and nonpolarized neutron matter (with $\Pi = 0$ at $H = 0$) as a function of the magnetic field strength for the BSk20 Skyrme force at $T = 15$ and $T = 30$ MeV and at two fixed densities $\varrho = 3\varrho_0$ and $\varrho = 4\varrho_0$. The meaning of the vertical arrows is the same as in Fig. 8(b).

with the matter contribution being $f_{Hm} = \frac{1}{\mathcal{V}}(E_m - TS) - HM$. The decrease of the Helmholtz free energy with temperature is, therefore, to be attributed to its matter part. Figure 11 explicitly shows this point.

An unexpected moment appears if we consider separately the behavior of the entropy of neutron matter with a generalized Skyrme interaction in a strong magnetic field. In Fig. 12, the difference between the entropy per neutron of magnetized neutron matter and that of the nonpolarized state (with $\Pi = 0$ at $H = 0$) is presented as a function of magnetic field at the temperatures $T = 15$ MeV and $T = 30$ MeV, and at the same densities as regarded above. It is seen that this difference is positive for all relevant magnetic field strengths. It looks like a spin-polarized state is less ordered than a nonpolarized state, contrary to intuitive assumption. In Sec. III, we showed that the unusual behavior of the entropy of a spontaneously polarized state is related to its dependence on the effective masses of neutrons with spin up and spin down and to the violation of the criterion (27). The entropy of magnetized neutron matter is given by the same general expression (17) and, after providing the low-temperature expansion, we would arrive at the same constraint (27) on the effective masses in a spin-polarized state guaranteeing that its entropy is less than that of the nonpolarized state. Figure 13 shows the left side D of the constraint (27) as a function of the magnetic field strength at the temperature $T = 15$ MeV, and densities $\varrho = 3\varrho_0$ and $\varrho = 4\varrho_0$, at which the accuracy of the approximation $T/\varepsilon_{F\sigma} \ll 1$ is acceptable. It is seen that the criterion (27) is violated and this explains the unusual behavior of the entropy of dense neutron matter in a strong magnetic field that is shown in Fig. 12.

Note that the unconventional behavior of the entropy of magnetized neutron matter with the Skyrme interaction was found earlier in Ref. [50]. The difference is that, for the SLy7 Skyrme interaction used in that work, a spontaneously polarized state appears already at zero temperature, while in the

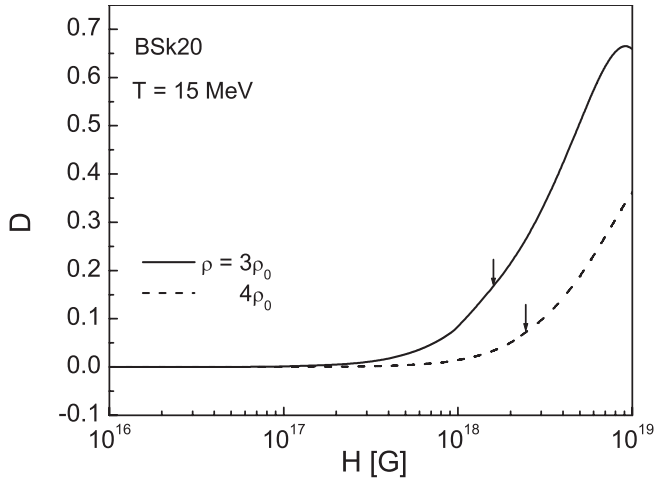

FIG. 13. Difference D in constraint (27) as a function of the magnetic field strength for BSk20 Skyrme force at temperature $T =$ 15 MeV and densities $\varrho = 3\varrho_0$ and $\varrho = 4\varrho_0$. The meaning of the vertical arrows is the same as in Fig. 8(b).

given research with a newly developed BSk20 Skyrme force, spontaneous polarization appears only at temperatures above the critical temperature. We have checked that the last feature is also characteristic for the BSk19 and BSk21 Skyrme forces. If to consider the appearance of a spontaneously polarized state as a weak point of a certain Skyrme parametrization (just this argument was used in Ref. [44] as the motivation for developing a new series of Skyrme forces), then this underlines the necessity to further concentrate the efforts on building a new generation of Skyrme forces being free of such kind of spin instabilities. Such an attempt was made in the recent article [59] by attracting ideas from nuclear energy density functional theory. However, the constraints obtained in this study on the Skyrme force parameters lead to the unrealistic consequence that the effective masses of nucleons with spin up and spin down in a polarized state should be equal, contrary to the results of calculations with realistic NN interactions [29,31]. On the other hand, the observational data still do not rule out the existence of a ferromagnetic hadronic core inside a neutron star caused by spontaneous ordering of hadron spins (in this respect, see, e.g., Refs. [60,61]). In any case, developed recently generalized Skyrme parametrizations BSk19–BSk21 are, currently, among the most competitive Skyrme forces for providing neutron star calculations and, certainly, are suitable for getting a qualitative estimate of the effects of pressure anisotropy in strongly magnetized neutron matter at finite temperature.

In summary, we have considered spin-polarized states in dense neutron matter in a model with the recently developed BSk20 Skyrme interaction at finite temperature under the presence of strong magnetic fields up to 10^{20} G. Although the BSk20 Skyrme force was thought up with the aim to avoid spontaneous spin instability at zero temperature, it has been shown that spontaneous instability appears at temperatures above the critical temperature, which is at least larger than 35 MeV. By this reason, we limited our consideration by the temperatures up to 30 MeV. For a spontaneously polarized state at finite temperature, the entropy demonstrates the unusual behavior being larger than that of the nonpolarized state. This feature has been related to the dependence of the entropy of a spin-polarized state on the effective masses of spin-up and spin-down neutrons and to the violation of some constraint on them at the corresponding densities and temperatures. In the strong magnetic fields considered in this study the total pressure in neutron matter becomes anisotropic. It has been shown that, for magnetic fields $H > H_{\rm th} \sim 10^{18}$ G, the pressure anisotropy has a significant impact on thermodynamic properties of neutron matter. In particular, vanishing of the pressure along the direction of the magnetic field in the critical field $H_c > H_{\rm th}$ leads to the appearance of the longitudinal instability of neutron matter. With increasing density and temperature of neutron matter, the threshold $H_{\rm th}$ and critical H_c magnetic fields also increase. In the limiting case considered in this study and corresponding to the density of about four times the nuclear saturation density and the temperature of about a few tens of MeV, the critical field H_c does not exceed 10^{19} G. This value can be considered as the upper bound on the magnetic field strength inside a magnetar. Our calculations show that the appearance of the longitudinal instability prevents the formation of a fully spin-polarized state in neutron matter, and only the states with moderate spin polarization can be developed. In the anisotropic regime, the field contribution to the Helmholtz free energy density becomes comparable and even dominates over the matter contribution. The longitudinal and transverse pressures and anisotropic EoS of neutron matter in a strong magnetic field have been determined at the densities and temperatures relevant to the interior of a magnetar. It has been clarified that the entropy of strongly magnetized neutron matter with the Skyrme BSk20 force demonstrates the unusual behavior similar to that of the entropy of spontaneously polarized state. In both cases, the same reason, discussed above, is responsible for such a behavior. The obtained results can be of importance in studies of cooling history and of the structure of strongly magnetized neutron stars.

ACKNOWLEDGMENTS

J.Y. was supported by grant 2010-0011378 from the Basic Science Research Program through NRF of Korea funded by MEST and by grant R32-10130 from the WCU project of MEST and NRF.

[1] R. C. Duncan and C. Thompson, Astrophys. J. **392**, L9 (1992).
[2] V. V. Usov, Nature (London) **357**, 472 (1992).
[3] W. Kluzniak and M. Ruderman, Astrophys. J. **505**, L113 (1998).
[4] K. Hurley, S. E. Boggs, D. M. Smith *et al.*, Nature (London) **434**, 1098 (2005).
[5] H.-Y. Chang and H.-I. Kim, J. Astronomy Space Sciences **19**, 1 (2002).
[6] C. Thompson and R. C. Duncan, Astrophys. J. **473**, 322 (1996).
[7] A. I. Ibrahim, S. Safi-Harb, J. H. Swank, W. Parke, and S. Zane, Astrophys. J. **574**, L51 (2002).

[8] S. Chakrabarty, D. Bandyopadhyay, and S. Pal, Phys. Rev. Lett. **78**, 2898 (1997).
[9] A. Broderick, M. Prakash, and J. M. Lattimer, Astrophys. J. **537**, 351 (2000).
[10] C. Cardall, M. Prakash, and J. M. Lattimer, Astrophys. J. **554**, 322 (2001).
[11] M. A. Perez-Garcia, Phys. Rev. C **77**, 065806 (2008).
[12] A. A. Isayev and J. Yang, Phys. Rev. C **80**, 065801 (2009).
[13] M. J. Rice, Phys. Lett. A **29**, 637 (1969).
[14] S. D. Silverstein, Phys. Rev. Lett. **23**, 139 (1969).
[15] E. Østgaard, Nucl. Phys. A **154**, 202 (1970).
[16] A. Viduarre, J. Navarro, and J. Bernabeu, Astron. Astrophys. **135**, 361 (1984).
[17] S. Reddy, M. Prakash, J. M. Lattimer, and J. A. Pons, Phys. Rev. C **59**, 2888 (1999).
[18] A. I. Akhiezer, N. V. Laskin, and S. V. Peletminsky, Phys. Lett. B **383**, 444 (1996); J. Exp. Theor. Phys. **82**, 1066 (1996).
[19] S. Marcos, R. Niembro, M. L. Quelle, and J. Navarro, Phys. Lett. B **271**, 277 (1991).
[20] M. Kutschera and W. Wojcik, Phys. Lett. B **325**, 271 (1994).
[21] A. A. Isayev, J. Exp. Theor. Phys. Lett. **77**, 251 (2003).
[22] A. A. Isayev and J. Yang, Phys. Rev. C **69**, 025801 (2004).
[23] A. A. Isayev, Phys. Rev. C **74**, 057301 (2006).
[24] V. R. Pandharipande, V. K. Garde, and J. K. Srivastava, Phys. Lett. B **38**, 485 (1972).
[25] S. O. Bäckmann and C. G. Källman, Phys. Lett. B **43**, 263 (1973).
[26] P. Haensel, Phys. Rev. C **11**, 1822 (1975).
[27] I. Vidaña, A. Polls, and A. Ramos, Phys. Rev. C **65**, 035804 (2002).
[28] S. Fantoni, A. Sarsa, and K. E. Schmidt, Phys. Rev. Lett. **87**, 181101 (2001).
[29] F. Sammarruca and P. G. Krastev, Phys. Rev. C **75**, 034315 (2007).
[30] F. Sammarruca, Phys. Rev. C **83**, 064304 (2011).
[31] G. H. Bordbar and M. Bigdeli, Phys. Rev. C **78**, 054315 (2008).
[32] M. Bigdeli, Phys. Rev. C **82**, 054312 (2010).
[33] D. Lai and S. Shapiro, Astrophys. J. **383**, 745 (1991).
[34] S. L. Shapiro and S. A. Teukolsky, *Black Holes, White Dwarfs and Neutron Stars* (Wiley, New York, 1983).
[35] Y. F. Yuan and J. L. Zhang, Astron. Astrophys. **335**, 969 (1998).
[36] E. J. Ferrer, V. de la Incera, J. P. Keith, I. Portillo, and P. L. Springsteen, Phys. Rev. C **82**, 065802 (2010).
[37] T. Tatsumi, Phys. Lett. B **489**, 280 (2000).
[38] G. H. Bordbar, Z. Rezaei, and A. Montakhab, Phys. Rev. C **83**, 044310 (2011).
[39] V. R. Khalilov, Phys. Rev. D **65**, 056001 (2002).
[40] A. I. Akhiezer, V. V. Krasil'nikov, S. V. Peletminsky, and A. A. Yatsenko, Phys. Rep. **245**, 1 (1994).
[41] A. I. Akhiezer, A. A. Isayev, S. V. Peletminsky, A. P. Rekalo, and A. A. Yatsenko, J. Exp. Theor. Phys. **85**, 1 (1997).
[42] A. I. Akhiezer, A. A. Isayev, S. V. Peletminsky, and A. A. Yatsenko, Phys. Lett. B **451**, 430 (1999).
[43] A. A. Isayev and J. Yang, in *Progress in Ferromagnetism Research*, edited by V. N. Murray (Nova Science Publishers, New York, 2006), p. 325.
[44] S. Goriely, N. Chamel, and J. M. Pearson, Phys. Rev. C **82**, 035804 (2010).
[45] B. Friedman and V. R. Pandharipande, Nucl. Phys. A **361**, 502 (1981).
[46] A. Akmal, V. R. Pandharipande, and D. G. Ravenhall, Phys. Rev. C **58**, 1804 (1998).
[47] Z. H. Li and H.-J. Schulze, Phys. Rev. C **78**, 028801 (2008).
[48] J. Rikovska Stone, J. C. Miller, R. Koncewicz, P. D. Stevenson, and M. R. Strayer, Phys. Rev. C **68**, 034324 (2003).
[49] Particle Data Group, C. Amsler *et al.*, Phys. Lett. B **667**, 1 (2008).
[50] A. A. Isayev and J. Yang, J. Korean Astron. Soc. **43**, 161 (2010).
[51] L. D. Landau, E. M. Lifshitz, and L. P. Pitaevskii, *Electrodynamics of Continuous Media*, 2nd ed. (Pergamon, New York, 1984).
[52] D. P. Menezes and C. Providência, Phys. Rev. C **69**, 045801 (2004).
[53] D. Vautherin and D. M. Brink, Phys. Rev. C **5**, 626 (1972).
[54] A. A. Isayev and J. Yang, J. Exp. Theor. Phys. Lett. **92**, 783 (2010).
[55] A. Rios, A. Polls, and I. Vidana, Phys. Rev. C **71**, 055802 (2005).
[56] A. A. Isayev, Phys. Rev. C **72**, 014313 (2005).
[57] A. A. Isayev, Phys. Rev. C **76**, 047305 (2007).
[58] R. C. Tolman, Phys. Rev. **55**, 364 (1939); J. R. Oppenheimer and G. M. Volkoff, *ibid.* **55**, 374 (1939).
[59] N. Chamel and S. Goriely, Phys. Rev. C **82**, 045804 (2010).
[60] P. Haensel and S. Bonazzola, Astron. Astrophys. **314**, 1017 (1996).
[61] M. Kutschera, Mon. Not. R. Astron. Soc. **307**, 784 (1999).